

ON THE RELATION BETWEEN STRUCTURE AND REACTIVITY IN THE CARBON
OXYGEN REACTION

D. Herein, J. Find, B. Herzog, H. Kollmann, R. Schmidt, R. Schlögl
Fritz Haber Institut der Max Planck Gesellschaft,
Faradayweg 4-6, D- 14195 Berlin, FAX -4930-8413-4401
H. Bartl
Institut für Kristallographie der Universität Frankfurt,
Senckenberganlage 30, D- 60054 Frankfurt,
Ch. Troyer
Institut für Analytische Chemie, Technische Universität Wien
Neubaugeb. 5/11 A-1070 Wien

Keywords: Mechanism of oxidation, single particle reaction, STM, X-ray absorption spectroscopy, X-ray diffraction, TG-MS analysis

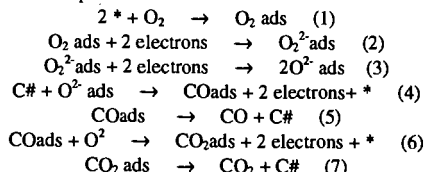
INTRODUCTION

The oxidation of graphite is a reference process for both generation of energy by combustion and for fundamental aspects of gas-solid interface reactions. The absence of large perfectly ordered crystals of graphite render rigorous model studies under surface science conditions very difficult despite the significant efforts in this area with large synthetic graphite surfaces(1). With integral kinetic techniques such as TPRS and instationary kinetic data a detailed mechanistic picture has been developed in a longstanding effort introducing a fraction of the geometric surface as active surface and the competition of two types of oxygen surface complexes which are either static and hence inhibiting or mobile and hence reactive in gasification(2,3,4). In addition, the selectivity to CO and CO₂ was traced back to different types of reactive surface intermediates with carbonyl or lactone structures respectively(5). The present contribution is an attempt to investigate the reaction with experiments aimed at selected atomistic aspects of the mechanistic picture. In a previous study the gasification of HOPG was found to procede at low temperatures (200 K) and low oxygen partial pressures (10⁻⁵ mbar) on suitably prepared surfaces (6). In this work as well as in many other reports(1,2,5) the importance of defects was pointed out which are either present in the substrate or may be created during reaction. In the model experiment (6) self-passivation occurred after very little conversion due to the creation of strongly adsorbed oxygen inhibiting low-temperature oxidation. The existence of strongly adsorbed oxygen and weakly adsorbed oxygen (2,3,7) in two different bonding geometries is a common ingredient to kinetic models of graphite oxidation.

Graphite oxidation is the prototype of a topotactic reaction proceeding only at the prism faces which should lead to a uniform shrinkage of the individual particles in uncatalysed reaction. Parallel to the recession mechanism there are basal plane defects which cause pitting corrosion creating additional prismatic faces during gasification and contribute in a difficult to control way to the overall rate. Other types of defects pin the edge recession e.g. by the occurrence of local sp³ bonding leading to a continous change in the length of the reaction interface and the creation of micro-hills (8) on reacting surfaces.

We used large flakes of RFL (0.5-1.2 mm dia.) and powders AF (3-1-µm dia.) natural graphite from Kropfmühl (Bavaria) which was purified from silicate and metal residues by basic melt and acid leaching. Standard gassification conditions were 20% oxygen in nitrogen and 927 K reaction temperature.

Modelling of the reaction is necessary to link macroscopic rate observations which are often severely affected by mass- and energy transport limitations with a minimum set of elementary step reactions describing the overall process:



These steps of reductive activation and carbon oxidation at a suitable defect(#) comprise the minimum number of reaction steps for the overall oxidation. It is evident that besides the reaction centre a second type of chemisorption site (*) is required for the reductive activation of oxygen which must exhibit an excess of delocalised electrons such as at the basal planes. These terrace sites are, however, unreactive for the nucleophilic activation product which implies the surface diffusion of the activated species. Some of these steps are different when homolytically activated oxygen from chemical or physical sources is involved (9). In this case, however, the topotactic reaction behaviour is lost. A key issue is the exact chemical nature and the location of the two types of active sites.

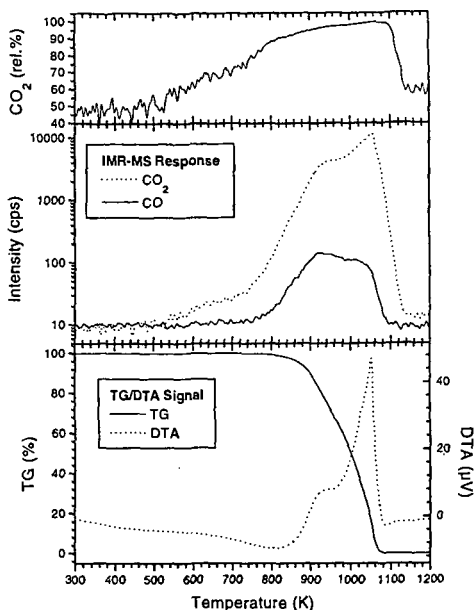


Fig.1: Selectivity, yield and TG/DTA response of an integral reaction experiment at standard conditions of a 0.5 cm bed composed of a 3:1 mixture of AF graphite with SiC powder in a coupled TG-IMR-MS experiment.

In Fig.1 we summarise macroscopic kinetic observations of a gassification experiment of AF graphite in an integral reactor. Sufficient dilution with silicon carbide ensured the presence of molecular oxygen at the reactor outlet at all temperatures applied. A special mass spectrometer of the IMR-MS ionisation type is applied for sensitive detection of CO and CO₂ without fragmentation overlap. Both the changes in selectivity and in rate (proportional to the DTA signal) indicate that the above reaction scheme is insufficient to explain the reaction progress in this case. The increase in CO₂ selectivity in the low-temperature regime complies with the initial removal of pre-formed C-O

insertion structures. The second increase in CO₂ at high conversion would mean that the insertion of active oxygen in suitably defective carbon-carbon structures becomes increasingly dominating over the addition of active oxygen onto unsaturated edge sites. This can be seen as consequence of the increasing abundance of mobile surface atomic oxygen (4) creating a high virtual pressure of oxygen. The di-oxygen partial pressure and the increasing abundance of basal plane sites (C*) increase with burn-off in contrast to the decreasing abundance of oxidation sites (C#) due to the recession of prismatic faces.

Changes in rate and selectivity with burn-off were also observed in isothermal macroscopic experiments which were found to be critical in quantitative reproducibility. Thus it was felt that single particle gassification experiments should be useful. The alternative, to use less active reagents or to drastically reduce the temperature, may lead to better kinetic data but may not describe the reaction in the same kinetic state as it is characteristic for a practical combustion, i.e. a different reaction step may be rate-determining at low rates (10) than at higher rates.

RESULTS

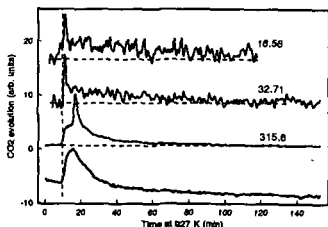


Fig.2: IMR-MS responses for single particle gassifications. The graphite weight in μg is used to designate the experiments. The top two traces refer to AF, the lower trace to RFL gassification. The unassigned trace is the water response for the RFL gassification. The vertical dashed line indicates the first time of constant oxygen partial pressure. At $t=0$ the heating in nitrogen was started. After reaching 927 K the gas was changed to oxygen in nitrogen. For the RFL experiment the oxygen was admitted in two steps at 11 and 20.5 min.

The simultaneous observation of the weight change and the gas evolution allowed to accurately fix the correct sample weight in single particle gassification experiments displayed in Fig. 2 which are heavily perturbed by buoyancy effects when starting the isothermal reaction after rapid heating in nitrogen. For AF oxidation a portion of the ceramic sample holder was dusted with graphite particles, for RFL single clean flakes (optical microscope) were used. In all cases after reaching a certain threshold partial pressure of oxygen a burst of reactivity occurred which was followed by a continuous activity at much lower level. For RFL graphite the threshold lies at about 5 vol% oxygen. Associated with the initial gassification is the desorption of water arising from oxidation of OH groups. The burst in reactivity is not connected with the creation of active sites from the OH group desorption as can be seen from the absence of a burst in the water trace. The data imply that an aged graphite surface is particularly reactive as the short duration of the burst excludes a location of the active centres underneath the surface.

The behaviour is reflected in the initial rates of reaction obtained from the weight change data. The observation that within the experimental accuracy both types of graphite with differing geometric surfaces gave comparable results indicates the integral character of the rate integrating over many processes and changes in local surface structure. Unexpected is the shape of the rate curve with time, as the initial gassification of a reactive surface followed by a steady state bulk reaction should not lead to a rate minimum which depends in its shape on type and mass of the graphite used. The characteristic time for reaching a constant rate is with about 120 min so long that a process of surface modification can be excluded. Moreover, comparison with the gas evolution data in Fig.2 reveals that the activity in gassification does not pass through a minimum but follows the expected behaviour. This implies that the weight change not only reflects the weight loss from gassification but indicates a simultaneous weight gain from the uptake of oxygen. Given that we are dealing with non-porous samples, the increase in weight cannot only be attributed to the formation of unreactive surface oxygen functions which can only cover a fraction of a monolayer (a monolayer of oxygen atoms on the geometric surface of a RFL flake would weigh about 0.002 μg , which is below the detection limit of the present experiment). We attribute the weight gain to the incorporation of oxygen in the bulk of the graphite sample. The effect is strongly dependent on temperature with a significant reduction in the detectable amount of incorporated oxygen with increasing temperature (less than 20% at 977 K compared to the amount at 927 K for RFL, for AF the effect is smaller than for RFL and so is the temperature dependence). The total amount of incorporated oxygen is with about 3 wt% of the RFL sample small enough to leave the question about its location in irregularities of the mosaic structure or as intercalate within the van-der Waals gaps of the regular crystallites. This will be discussed below.

STM can be used to reveal local details of the oxidation mechanism of graphite (8,11) as the reaction does not produce -as in metal oxidation reactions- scales of low electric conductivity. The extra high sensitivity of STM to roughness allows to image deviation from a planar surface with a sensitivity of 2-3 orders of magnitude higher than the lateral resolution of a survey image. This is illustrated in Fig.3 showing a RFL flake before gassification and the same flake after 20 % burn-off. The outer surface of the flake is rather irregular and exposes a high abundance of prismatic faces in form of micro-flakes sitting on top of the main particle. After partial gassification these micro flakes have all disappeared leaving a smooth surface with a considerably lower basal-to prism face ratio. It is noted that none of the steps seen in this image are monosteps. The minimum height is 3 steps and only odd numbers of graphene layers were observed to constitute these stable edges. The impression of the regularity is adventitious, there are many situations with irregular edges on the over 1200 images which were analysed. The different appearance of the steps in different directions is due to the uneven shape of the STM tip used for imaging. These tips have to be extra coarse in order to survive the frequent crashes which are unavoidable in imaging such rough surfaces. From these images it becomes apparent why gassification starts with a high initial rate as the intermixing of the two active centres of planar basal planes for oxygen activation and of rough prism faces for oxidation is much better than after removal of the microflakes. The images fit well to the integral observations of the rate measurements. The triangular rows in image 3C indicate the local interruption of the surface electronic conductivity by firmly held adsorbates such as strongly bound oxygen atoms decorating lines of defects in the partly gassified crystal. Ribbons of dislocations which are normally detected by TEM contrast (12) are exposed to atomic oxygen and provide centres for stable functional group formation. The absence of atomic resolution in oxidised areas can further be seen in image 3D which shows the rare situation (8 out of 1200) of the co-existence of insulating islands of non-graphitic nature such as „carbon oxide“ or diamond-like carbon with normal surfaces separated by a double- and single-atomic step structure. These two latter images reveal the presence of lines and areas of basal planes which are non-graphitic in character and provide evidence for a local chemical heterogeneity.

Imaging monoatomic steps on graphite is rarely possible on cleaved surfaces. On oxidised surfaces it is, however, possible in particular at monoatomic etch pits. Fig.4A shows a situation in which a top crystallite exhibits a 120 deg edge while sitting on a monoatomic step. At this level of resolution the high degree of orientation along crystallographic main directions can be seen in areas with low defect density. Most remarkable is the different appearance of the two prism faces (triatomic step height) in two different directions. The analysis of the effect as function of the STM parameters reveals that the „structure“ in one prism face is an artefact caused by the absence of electrical conductivity. This precludes imaging of the atomic arrangement but reveals that the local chemistry of the two prism face orientations is different with the structured face being largely covered by covalently bound oxygen groups. The other edge seems to be free of insulating bonds and may thus represent a more reactive face. These assignments are speculative as the observations are not possible during gassification (4). It remains, however, the evidence for a local difference in chemical interaction of differently oriented prismatic faces.

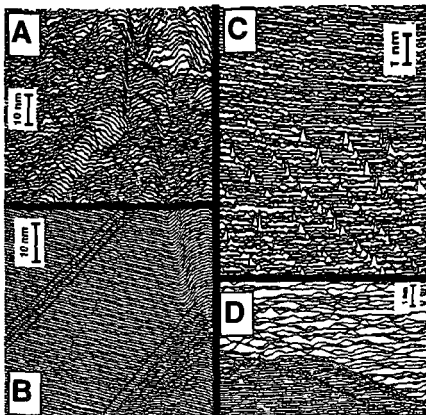


Fig.3: STM wide scans over a flake of RFL graphite before oxidation(A) and after 20% burn-off (B,C;D). A Burleigh ARIS 6000 instrument with a W tip was used: gap voltage + 50 mV, constant current 1.0 nA, raw data as line scans. Scan areas are: A,B: 300x300 nm, C: 500x500 nm, D: 50x50 nm

In image 4B the atomic resolution is illustrated of oxidised steps near a terminating basal plane defect. Two top graphene layers are sitting in different rotation angles relative to the supporting graphene layer. The fuzzy appearance of the steps is also due to an imaging artefact caused by a low electrical conductivity at the step edges. The striped appearance is a sign of the tip crashing into the step and requiring to travel over several atomic distances behind the steps to reach stable tunnelling

conditions again. This is a strong indication of the presence of localised electronic states at the step edges and the absence of radicals or delocalised states at these locations. The presence of carbon-heterobonds (oxygen or hydrogen) is the likely explanation

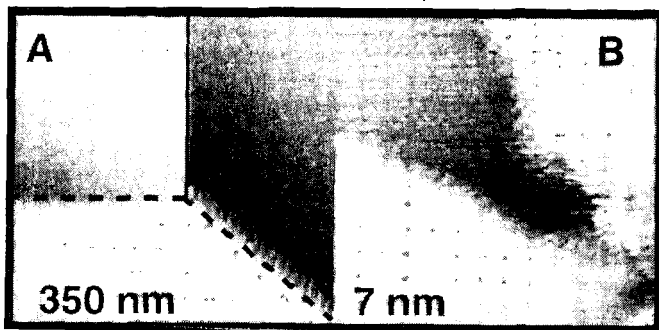


Fig.4: STM images of RFL after 50 % burn-off. In image A the dashed lines denote the contours of a top crystallite sitting over a plane with a monoatomic step (full line). In B the atomic resolution is achieved for oxidised monoatomic steps. The figures denote the lateral image size, the step heights were determined from profile scans (not shown). The imaging conditions were as in Fig.3.

which allows to experimentally support the chemical notion that the terminating graphene edges are the places of interaction between carbon and oxygen. This image reveals a possible zone of reactivity for addition (edges) and insertion (rows of atoms right behind the step) of activated oxygen. The formation of islands of modified carbon atoms within basal plane terraces as a consequence of gassification was not observed indicating that the spontaneous creation of gassification sites within perfect graphene sheets does not occur. This follows also from thermodynamics as the creation of the very first single vacancy requires 676 kJ/mol energy (13) whereas the produced CO₂ molecule contributes only 393 kJ/mole to the energy balance. The creation of vacancies becomes rapidly easier with defects already present (13). The necessity to have already an interruption in the graphene layer for the oxidation to proceed, drives the reaction to clean basal planes (11) and to a topotactic progression along prism faces and along „a-priori“ defect sites (4,14).

We failed to detect islands of oxygen at the terraces of the basal planes as they are seen in metal-oxygen interaction studies. This implies that the interaction of oxygen with the basal planes which is required for its activation is too weak to allow imaging by STM or that the STM tip field is sufficient to clear the imaging area on the basal planes. We have shown by TDS that both water and oxygen are adsorbed on basal planes and that the failure to see these adsorbates is an STM artefact(8).

X-RAX DIFFRACTION EXPERIMENTS

For the observation of a gas-solid interface reaction the bulk-sensitive technique of X-ray diffraction should not provide any useful data as the reacting surface is not probed by the

experiment. In continuation of our single particle analysis of the reaction we studied RFL flakes by Laue photographs as function of burn-off. The results are summarised in Fig.5.

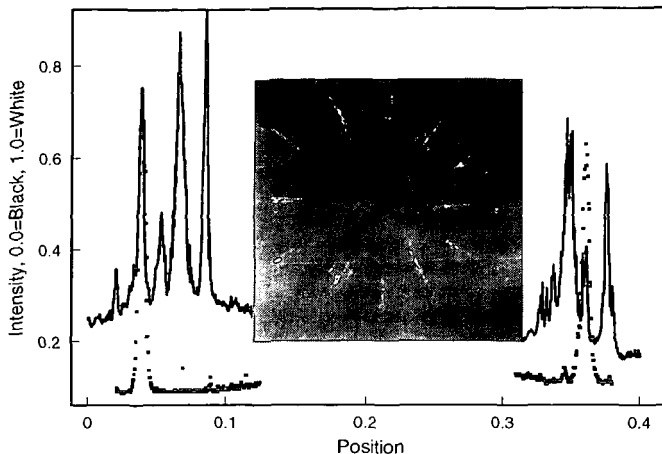


Fig.5. Laue Photographs ($Mo\ K\alpha$ radiation, beam parallel to the c -axis) of a RFL flake before oxidation (top densitometer trace and photograph) and after 20 % burn-off (bottom densitometer trace). It emerges very clearly that the flake was polycrystalline in (hk) orientation and became almost perfectly single crystalline after partial oxidation.

The data show that the flake was liberated from small crystallites throughout its volume. Moreover, the mosaic crystallites constituting the main part of the flake became better aligned in the basal plane (sharp profile after partial oxidation). This observation is corroborated by the fact that Laue patterns (parallel a,b) showing the stacking order could not be obtained before oxidation but revealed a high degree of AB stacking after partial burn-off. This indicates that partial oxidation causes a kind of „chemical annealing“. The most defective crystallites will be burnt away preferentially and so will be interstitial carbon in the interior of the mosaic crystal. This requires the action of oxygen not only on the geometric surface but also at the inner surfaces of defective regions. This is seen in parallel to the small but detectable storage of oxygen in the initial phase of oxidation. We would thus locate the oxygen not as an intercalate in between the graphene galleries but rather as „bubbles“ located at defects.

In-situ powder diffraction studies of the (002) reflection under standard gassification conditions were performed in order to support this interpretation. Intercalation, even in small quantities should lead like in ROSIG compounds to a splitting and broadening of the (002) reflection. Initial experiments with HOPG as sample and Si as internal standard seemed indeed to support the notion about the residual intercalation (15). Frequent repetition of the experiment in different diffractometer geometries and with different graphite materials revealed, however, that the observed drastic changes in lineprofiles are diffraction artefacts caused by the uncontrolled sample movement exposing differently misaligned sections of the mosaic crystal to the diffraction condition. The lineprofile became increasingly symmetric and significantly narrower with progressing oxidation after removing this artefact. This is exemplified in Fig.6 The unsteady course of the difference curve at low temperatures indicates the residual positioning problems of the RFL sample. A persistent reduction of the linewidth close to the instrumental limit was observed after oxidation and cooling back to 300 K. The lattice constant was also observed to shrink irreversibly after oxidation from the value of the Ar experiment which was found to be 340.12 (± 0.03) pm at 873 K. The selectivity was also found to change with the structural parameters. The excess of CO_2 formation increased in parallel with the reducing FWHM and with the change in lattice spacing. In particular, the onset of all changes co-occurred in all experiments suggesting a correlation of the effects. The defective structural parts gassify preferentially to CO , the better ordered graphitic carbon reacts preferentially to CO_2 .

X-RAY ABSORPTION SPECTROSCOPY

The average local electronic structure is an important parameter in the reactivity scenario of the gassification as it provides information about the action of the di-oxygen activation as rate-determining step. XPS was found to be rather insensitive to the variation of carbon-carbon bonding within one type of graphite partly because of the photoemission physics and partly because of the ill-defined surface-sensitivity (16). This fact can be used advantageously in performing photoabsorption experiments at the carbon 1s edge using synchrotron radiation. In this experiment the insensitive photoemission process is the initial state allowing thus to interpret the spectra without having to account for initial state changes. The general shape of the spectra which allow clearly to discriminate π^* states from σ^* states has been discussed elsewhere (16, 17). In Fig.

7 some quantitative data about the π^* states are collected. A sample of HOPG was used for the reference experiment shown in the top panel. The changes in the polarisation of the π^* resonance

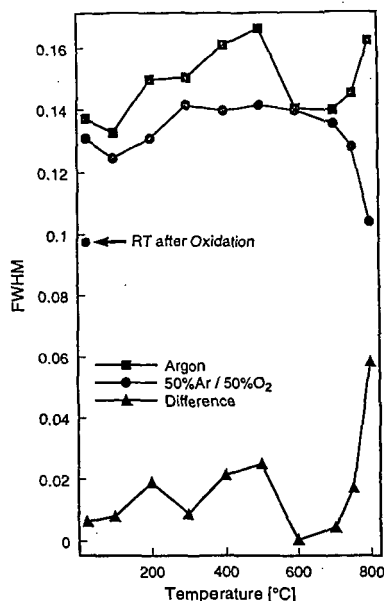


Fig.6: Evolution of the FWHM of the RFL graphite (002) reflection as function of in-situ treatment temperature. The data were obtained from Gaussian lineprofile fits. The difference plot proves the action of oxygen and not of temperature in the annealing procedure. The data were recorded after reaching steady state conversion at each temperature point in the oxidation scan and after 2h waiting under Ar respectively.

are compared for pristine, oxidised and Ar ion sputtered surfaces. Oxidation causes mainly a surface roughening by pitting giving rise to the small loss in polarisation at low angles between the light beam and the sample basal plane. The average electronic structure is, however, not different between pristine and oxidised graphite indicating that oxidation proceeds on few sites on the surface and does not cover the surface with intermediate C-O groups. This precludes a significant reaction-induced increase in defect abundance. Sputtering of graphite with Ar ions destroys the surface and breaks many sp^2 bonds leaving a electronically highly disordered surface (18). This can also be seen drastically from the change in

polarisation behaviour which indicates the loss of preferred orientation of the π^* orbitals (reduced slope) and the loss in abundance of sp^2 centers (smaller absolute value at high angles). This type of surface serves as model for a type of defects inhibiting oxidation by removing the delocalised electronic states required for the first three steps in the oxidation sequence. The fact that such an isotropic attack of the surface electronic structure does not occur during oxidation is a microscopic confirmation of the topotactic nature of the reaction requiring for its progression minority surface sites which are not located within the basal plane.

This technique is also suited to follow the evolution of the graphitic character with burn-off by examination of the intensity of the π^* resonance normalised to the carbon content as shown in the lower panel of Fig. 7. Changing the detection condition from total Auger yield to partial Auger yield allows to probe non-destructively the electronic structure depth-selective. The data show that with increasing burn-off the degree of graphitic surface increases both at the surface (topmost atomic layer) and in the bulk (some 10 nm). This is full in line with all other observations reported here and shows for a large area the „cleaning“ effect detected by STM. It further shows that the oxidative bulk annealing reduces in the initial stage of gasification the abundance of non-graphitic carbon atoms.

CONCLUSIONS

The microscopic informations presented corroborate in general the traditional view about the reaction mechanism as a topotactic gas-solid reaction with two different active sites having to interact for efficient reaction. The prism faces seem to be chemically different according to their crystallographic orientation. They are, however, clearly the sites of carbon-heterobond formation. The consequence of the step is a pronounced modification of the electronic structure of the carbon atoms near the edge. These observations call for a structure-sensitivity of the reaction at different location of the active sites (e.g. variation after equations (5) and (6) of the mechanism). This would be in line with the picture of oxygen addition and insertion as being the elementary steps defining the selectivity. The conjecture that one of these reaction sites would mainly not be located near prism edges or „a-priori“ defects is not supported by the data presented. The high thermal stability of the carbon heterobonds on an intact long-range-ordered prismatic edge (see Fig. 4) requires the overall high reaction temperature of the gasification in order to achieve steps (5) and (7) of the reaction sequence. Higher disordered reaction interfaces with an average lower carbon coordination number are beneficial for a lower reaction temperature or a higher rate (Fig. 3).

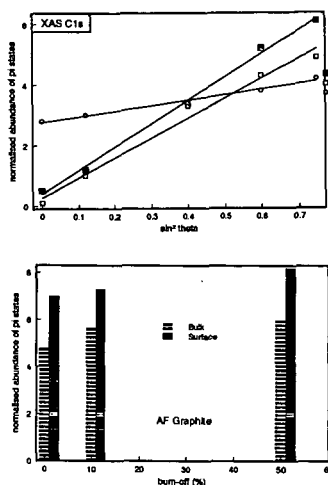


Fig. 7. Top: Angular dependence of the intensity of the 286 eV π^* resonance for differently prepared HOPG surfaces. Oxidation was performed in-situ under standard conditions which created a large amount of etch pits. Ar ion bombardment was carried out at 1 kV and 10-4 mbar Ar for 2 min. XAS data were recorded in the total yield mode at the HE PGM II station at the BESSY synchrotron. The bottom panel shows the evolution of the π^* intensity with burn-off for AF graphite (external sample preparation). Surface sensitivity is created by comparison of total yield (0 eV, bulk) and partial yield (150 eV, surface) data.

The single particle experiments further gave evidence for the preferential burn-off of small crystallites with high initial rate covering the individual flakes. This process drives the reaction towards a state in which activation of chemisorbed di-oxygen according to reactions (1)-(3) is not rate-determining despite the overall small sticking coefficient of di-oxygen on graphite (001). This is taken as strong

indication that the well-ordered basal planes provide active centers for reductive di-oxygen dissociation and exhibit a function in the gassification mechanism.

Incorporation of oxygen into graphite in weighable amounts was detected which is likely to be located in the voids of the mosaic crystal. It was not possible to produce unambiguous structural evidence for regular intercalation of oxygen as islands between graphene layers. At the „internal“ surfaces the oxygen removes preferentially lattice defects which allow oxidation-induced low-temperature annealing of the graphite crystal. The effect was detected by X-ray diffraction methods and by the observation of the action of mechanical forces providing activation energy for defect ordering (see Fig. 3 C). Careful oxidation of natural graphite flakes can lead to well-ordered samples.

Defects act on the gassification rate as promoters by interrupting the long-range electronic structure of the graphene edges or within the planes (pitting) without destroying the local electronic structure (Fig. 7) or as inhibitors by pinning the delocalised valence electrons within a few interatomic distances. The counteraction of these irregularities gives rise to an unpredictable rate of individual mosaic flakes. The generation of a sufficient number of defects to modify the surface electronic structure as detectable by a (small) change in average hybridisation or structural roughening was not observed.

ACKNOWLEDGEMENTS

Financial support came from the Otto Röhm Foundation and the Fonds der Chemischen Industrie.

REFERENCES

- (1) S.R. Kelemen, H. Freund, *Carbon* **23**, (1986), 619
- (2) P.L. Walker jr., R.L. Taylor, J.M. Ranish, *Carbon*, **29**, (1991), 411
- (3) J.A. Moulijn, F. Kapteijn, *Carbon*, **33** (1995), 1155
- (4) J.M. Ranish, P.L. Walker jr., *Carbon*, **31**, (1993), 135
- (5) R.N. Smith, D.A. Young, R.A. Smith, *Trans. Faraday Soc.*, **62**, (1966), 2280
- (6) R. Schlögl, G. Loose, M. Wesemann, *Solid State Ionics*, **43** (1990), 183
- (7) B. Henschke, H. Schubert, J. Blöcker, F. Atamny, R. Schlögl, *Thermochimica Acta*, **234** (1994), 53
- (8) R. Schlögl, F. Atamny, J. Wirth, J. Stephan, *Ultramicroscopy*, **42-44**, (1992), 660
- (9) H. Marsh, T.E. O'Hair, R. Reed, *Trans. Faraday Soc.*, **61**, (1965), 285
- (10) I.M.K. Ismail, P.L. Walker jr., *Carbon*, **27**, (1989), 549
- (11) L. Porte, D. Richards, P. Gallezot, *J. Microscopy*, **152**, (1988), 515
- (12) M.M. Heerschap, P. Delavignette, *Carbon*, **5**, (1967), 383
- (13) A.P.P. Nicholson, D.J. Bakon, *Carbon*, **13**, (1974), 275
- (14) C. Roscoe, J.M. Thomas, *Proc. Roy. Soc., A, London*, **297** (1966), 397
- (15) B. Herzog, D. Bokern, Th. Braun, R. Schlögl, *Proc. EPDIC-3, European Conf. Powder Diffraction*, (1993), 3
- (16) F. Atamny, J. Blöcker, B. Henschke, R. Schlögl, Th. Schedel-Niedrig, M. Keil, A.M. Bradshaw, *J. Phys. Chem.*, **96**, (1992), 4522
- (17) R. A. Rosenberg, P.J. Love, V. Rehn, *Phys. Rev., B*, **33**, (1986), 4034
- (18) R. Schlögl, *Surf. Sci.*, **182**, (1987), 861